Impact of injector characteristics on combustion instabilities in a swirl-spray combustor

Preethi Rajendram Soundararajan, Guillaume Vignat, Daniel Durox, Antoine Renaud, Sébastien Candel

Noname manuscript No.
(will be inserted by the editor)

Impact of injector characteristics on combustion instabilities in a swirl-spray combustor

Preethi Rajendram Soundararajan · Guillaume Vignat · Daniel Durox · Antoine Renaud · Sébastien Candel

Received: date / Accepted: date

Abstract The influence of the injection system on combustion instabilities is investigated in this work by making use of systematic experiments with three swirlers having similar geometries, but different pressure losses and swirl numbers. The swirling injectors are tested in a laboratory-scale swirl-stabilized combustor called SICCA-spray that represents one segment of the MICCA-spray annular combustor. Measurements are performed with liquid heptane fuel, delivered as a hollow cone spray by a pressure atomizer. Self-sustained oscillations are examined for the different swirlers by varying the chamber length. Test results show differences in oscillation frequency and oscillation amplitude between the different swirlers. Acoustic damping estimated for each swirler under cold flow conditions reveal their distinct behavior. This, however, is not enough to explain the differences observed in the unstable behavior of the various systems. .

Keywords Combustion instability, injector dynamics, spray-swirl combustor, self-sustained instabilities, damping.

1 Introduction

In aeronautical applications and gas turbines for energy production much of the research in combustion dynamics has concentrated on configurations operating in a nearly premixed mode, in which the flame is anchored by a swirl injector. These swirled injectors produce relatively compact flames that feature a large volumetric power in an environment characterized by a reduced level of damping, thus making the system more susceptible to combustion instability [1]. Investigations of swirling flames dynamics (see the reviews by [2,3]) indicate that the injection unit plays a major role in this respect and determines the dynamics of the system and its propensity to instability. In the broad variety of injection configurations, one may try to distinguish swirling units in terms of characteristic parameters, the most obvious being the swirl number S and the pressure drop Δp or the relative pressure drop $\Delta p/p_0$ (in addition to other parameters like the Reynolds number or the turbulence intensity at the injector outlet). By comparing injectors featuring different swirl numbers and pressure losses the present investigation intends to underline the role of the swirling injection unit in the process leading to self sustained oscillations. Research reported in this article is only one part of a more comprehensive effort to understand the role of injectors by examining the flame describing functions of different units and by identifying the role of the injector admittance in fixing conditions of instability.

At this stage it is worth briefly reviewing some previous investigations that specifically discuss effects of swirling injector parameters on combustion dynamics. One interesting indication on the key role of the swirl number is provided by the large eddy simulation (LES) of a swirl-stabilized, lean premixed combustor reported by [4]. For the swirl arrangement (referred as premixer) considered,

EM2C lab, CNRS and CentraleSupelec, University Paris-Saclay, 91192 Gif-sur-Yvette, France
E-mail: preethi.rajendram-soundararajan@centralesupelec.fr
Present address of G. Vignat: Stanford University Department of Mechanical Engineering, Stanford, CA 94305, USA.

an increase in swirl number from 0.56 to 0.84 causes a 50% reduction in the amplitude level. Another LES focused on the effect of swirl on flame dynamics in a lean premixed swirl-stabilized combustor [2] indicates that the variation in swirl number has a preferential oscillation behavior; a strong swirl favors transverse acoustic oscillations whereas longitudinal oscillations dominate the case of weak swirl. The effect of swirl number is made evident in [5] which makes use of a swirler with variable swirl number. The blades' stagger angle in the swirler is controlled by an electric motor allowing systematic scanning of stable and unstable regimes. Two types of instabilities are uncovered, one with a higher frequency occurring for larger values of the swirl number and featuring the highest values of acoustic pressure; and another coupled with the plenum at lower values of swirl number. In a more recent investigation, [6] considers the instability mechanism in an industrial-scale lean premixed gas turbine combustor with a swirling injection unit. A part of this study involves analyzing the effect of swirl number variations (two swirlers with swirl numbers 0.4 and 0.8) on self-sustained oscillations, which was characterized by varying the combustor length. In the higher swirl number case, the normalized pressure amplitude as well as the heat release rate fluctuations were more intense than those corresponding to the low swirl number situation. These experimental results are somewhat at variance with those described in [4]. The fact that these studies lead to opposing conclusions may be interpreted as an indication that the instability depends mainly on the flame dynamics and its coupling with acoustics, but not directly on the swirl number value. While many previous research was mainly focused on the swirl number influence, a recent work by [7] considers effect of injector pressure loss on self-sustained oscillations. Measurements carried out on a single injector swirl-spray combustor operating with liquid fuel indicate that a variety of instability regimes occur when the operating conditions are varied. It is shown that the pressure drop has a notable influence on the stability of the system, as well as on the intensity and nature of the unstable oscillations. Further indications on the influence of the injection units are also provided by experiments on annular combustors carried out in the recent period on a laboratory scale facility MICCA-spray [8,9].

It appears from this brief review that, in swirl-stabilized flames, the injector defines to a large extent the combustion dynamics of the system. Changes in injector characteristics in the form of varying swirl number could alter the flow behavior resulting in a different flame shape. Variations in the pressure drop across the injector (leading to a change in injector impedance) may alter the coupling between plenum and chamber, modifying the instability behavior thus motivating the present investigation. In the current study, a single sector system is employed to understand the effect of injector on combustion instabilities under longitudinal self-sustained oscillations. Data originating from a single sector configuration may usefully guide investigations on multiple injector annular configurations, a methodology that is exemplified by [10]. In this brief article, the experimental setup of SICCA-spray system is described in section 2. Experimental results gathered in the subsequent sections illustrate differences in self-sustained instabilities (section 3) and damping rates (section 4) that may be observed in the laboratory-scale combustor equipped with different swirlers.

2 Experimental setup

Experiments are carried out in a single sector set-up (SICCA-spray) representing a segment of the laboratory-scale annular combustor, MICCA-spray. The experimental setup shown schematically in Fig. 1 consists of a plenum connected to the chamber through a spray-swirl injector. Liquid heptane (fuel) is supplied through a central tube in the plenum and its mass flow rate is set by a Bronkhorst CORI-flow controller with a relative accuracy of 0.2%. The fuel is delivered into the chamber as a hollow cone spray by a simplex atomizer producing a dispersion of fine fuel droplets. Air at atmospheric conditions is supplied at the bottom of the plenum by means of a Bronkhorst EL-FLOW mass flow controller with a relative accuracy of 0.6%. Air from the plenum enters the chamber through an injection unit. It contains an air distributor leading to a tangential swirler with six channels. The passage of air through the swirler channels results in a clockwise rotation of the incoming flow. The flow delivered by the swirler enters into the combustion chamber through a conical section with an 8 mm diameter outlet. Three swirlers are used in this study, designated as 707, 712 and 716. The pressure drop Δp across the injector, the head loss coefficient σ, and the swirl number S are gathered in Tab. 1. The swirlers 707 and 712 have almost the same swirl

Table 1: Characteristics of the swirlers used in the present study measured in an unconfined SICCA-spray in cold flow with an air mass flow rate of $\dot{m}_{\text{air}} = 2.6\,\text{g}\text{s}^{-1}$. The measurements for the swirl number S is made at a distance of $x = 2.5\,\text{mm}$ above the backplane. The head loss coefficient σ is calculated using the equation $\Delta p = \frac{1}{2}\rho_0\sigma\overline{u}$ where $\overline{u}$ is given by $\dot{m}_{\text{air}}/\pi\rho_0 R_{\text{inj}}^2$ and is equal to $43\,\text{m}\,\text{s}^{-1}$. Here $R_{\text{inj}} = 4\,\text{mm}$, the radius of the injector outlet. Adapted from [11].

Swirler	S (-)	Δp (kPa)	σ (-)
707	0.60	3.65	3.33
712	0.59	4.50	4.10
716	0.70	5.74	5.23

Table 2: Details of the various experimental measurements.

Measurement	Method	Sensor details	Acquisition
Self-sustained instability	– Varying the chamber length from 165 mm to 365 mm in steps of 50 mm – Measurement with flame	– Pressure measured by microphone MC1 at chamber backplane – Mounted on the waveguide at a distance of 276 mm, propagation delay 0.78 ms – Brüel & Kjær 4938 microphones with type 2670 preamplifiers	– Sampling rate $f_s = 16{,}384$ Hz – Sampling time $t_s = 8\,\text{s}$
Flame images	– OH* chemiluminescence – Measurement with flame	– Intensified CCD camera – PI-MAX from Princeton instruments	30 frames are averaged to obtain a single image
Damping	– Pulsing from the top of the combustor with a driver unit – Frequency sweep from 300 Hz to 600 Hz at the rate of $1\,\text{Hz}\,\text{s}^{-1}$ – Measurement in cold conditions	– Pressure response (p_c) measured by microphone MC1 – Reference microphone (p_{ref}) measures frequency response of driver unit	– Sampling rate $f_s = 16{,}384$ Hz – Sampling time $t_s = 2\,\text{s}$ at each frequency block

number and velocity profile, but 712 has a higher pressure drop. The 716 swirler has a higher value for both swirl number and pressure drop. The readers are referred to Vignat et al. [11] for a detailed characterization of swirlers, velocity profiles and of the droplet spray. In the present

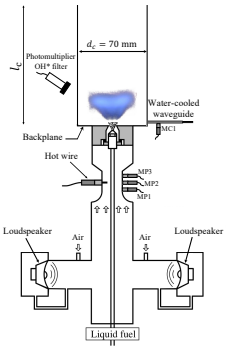

Fig. 1: Schematic of the experimental setup of SICCA-spray.

investigation, the burner is operated at a global equivalence ratio $\phi = 0.85$ which corresponds to an airflow rate of $2.6\,\text{g}\,\text{s}^{-1}$ and a fuel flow rate of $520\,\text{g}\,\text{h}^{-1}$. The combustion chamber consists of two sections, each with an internal diameter of 70 mm: a bottom metal ring of length 15 mm supporting the water-cooled waveguide of microphone MC1 and a top section formed by a fully transparent cylindrical quartz tube providing complete optical access to the combustion zone. The details of the different experiments described in this paper are tabulated in Tab.2.

The shape of the flames formed by each injection system is shown in Fig. 2 under stable conditions. The flame shapes corresponding to the various swirler units are notably different. For

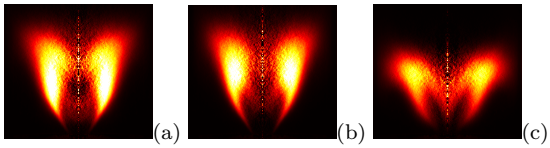

(a) (b) (c)

Fig. 2: Flame images in SICCA-Spray showing the flame chemiluminescence (OH*) captured using an intensified CCD camera. The images are captured at a chamber length of 100 mm when SICCA-spray is stable. An Abel transform is applied to the captured images. (a) 707, (b) 712, (c) 716.

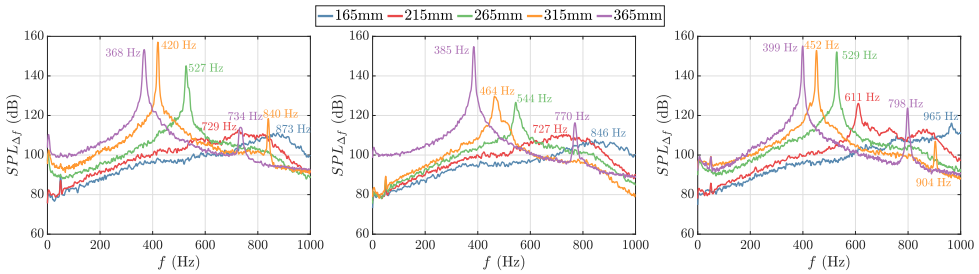

(a) 707 (b) 712 (c) 716

Fig. 3: Frequency spectrum showing SPL for the three swirlers at different operating lengths of SICCA-spray.

707, the flame is relatively narrow and takes a "V-Shape". For 712, the "V" shape opens up a little while the flame corresponding to 716 spreads out and takes the form of a hollow "M" with a central trough –a feature that may be attributed to the higher swirl induced by this swirler.

3 Self-sustained instabilities

To examine the instability characteristics of SICCA-spray under self-sustained oscillations, it is instructive to vary the chamber length l_c. Five different chamber lengths are considered from 165 mm to 365 mm, increasing in steps of 50 mm. A separate measurement is performed at 115 mm which serves as a reference for comparing the measurements taken at other lengths as there is no instability at this length. The measured chamber pressure fluctuation at 115 mm is $p^{bl}_{\mathrm{rms}} = 67\,\mathrm{Pa}$ which is due to the background combustion and flow noise and is used as a baseline for comparing the instabilities at other chamber lengths.

The acoustic pressure power spectrum is calculated using Welch's periodogram method considering 32 Hamming windows and a 50% overlap between windows resulting in a frequency resolution $\Delta f = 4\,\mathrm{Hz}$. The root mean square (rms) of the chamber pressure measured by MC1 represents the instability amplitude dubbed p_{rms}. Together the peak frequency f_{peak} obtained from the frequency spectrum, they characterize the self-sustained oscillations of SICCA-spray. Fig. 3 shows the power spectrum plotted in terms of sound pressure level, $SPL_{\Delta f}$ in the frequency band Δf and given in dB (the reference pressure being $p_{\mathrm{ref}} = 2\,10^{-5}$ Pa). Based on the instability amplitude the system is considered to be either stable or unstable using two criteria. A first condition to identify an unstable regime is that the pressure rms value be at least twice that recorded in the baseline configuration $p^{bl}_{\mathrm{rms}} = 67\,\mathrm{Pa}$, ie that $p_{\mathrm{rms}} > 2\,p^{bl}_{\mathrm{rms}}$. In the second condition, the maximum $\mathrm{SPL}_{\Delta f}$ in the spectrum (Fig. 3) is compared with the maximum $\mathrm{SPL}^{bl}_{\Delta f}$ ($\approx 100\,\mathrm{dB}$) recorded in the baseline configuration ($l_c = 115\,\mathrm{mm}$) and one may require that the maximum peak level should exceed the baseline level by a predetermined amount, typically $\Delta\mathrm{S} = 30\,\mathrm{dB}$. This condition may be written as $\mathrm{SPL}_{\Delta f}(peak) > \mathrm{SPL}^{bl}_{\Delta f}(peak) + \Delta\mathrm{S}$. If the two conditions are met, one may say that the system is unstable but when only one condition is fulfilled, the system is considered to be mildly unstable. Fig. 4 shows the stability map of SICCA-spray for the different chamber lengths based on these criteria. Additionally, the peak frequency f_{peak} and pressure amplitude p_{rms} for the different chamber lengths are shown in Fig. 4. For 707, at $l_c = 165\,\mathrm{mm}$ and 215 mm, the system is stable as there is no peak in the frequency spectrum and p_{rms} is low. These points are represented as black stars in Fig 4. At the other lengths, SICCA-spray with 707 is unstable marked by an

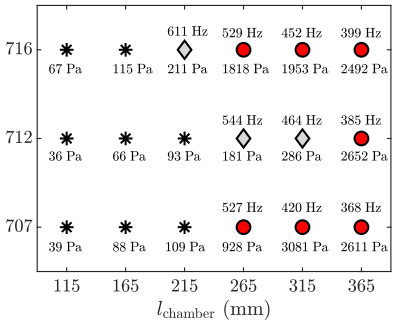

Fig. 4: Instability map of SICCA-spray at different chamber lengths l_c for the different swirlers. The black stars represent the stable points, black diamond with gray shading represent the points that are mildly unstable, and black circles with red shading represent the unstable points. The peak frequency from the frequency spectrum f_{peak} (Hz) and rms chamber pressure P_{rms} (Pa) from MC1 is indicated for each configuration.

evident frequency peak and significantly higher values of pressure amplitude —denoted by black circles with red shading. With 712, the system is stable at $l_c = 165$ mm and 215 mm which can be deduced from the absence of a peak in the frequency spectrum of Fig. 5b and it exhibits a behavior similar to that of 707 at this length. However at $l_c = 265$ mm and 315 mm, SICCA-spray is only mildly unstable, a behavior that differs from that found for 707 at these lengths. At $l_c = 365$ mm, the instability reaches a level similar to that of 707 but it occurs at a frequency of 385 Hz, which is higher than that of the instability frequency of 707 (368 Hz). For 716, the only stable configuration is at 165 mm. At $l_c = 215$ mm, the system features a small peak in the frequency spectrum and the pressure amplitude p_{rms} is moderate. Consequently, SICCA-spray is mildly unstable at this point —represented by a black diamond with gray shading in Fig 4. At the other lengths ($l_c = 265, 315$ and 365mm), SICCA-spray is unstable with high chamber pressure amplitudes. These results of the longitudinal self-sustained instabilities show that changing the swirler can have an impact on both amplitude and frequency of instability.

4 Damping rate

To determine the stability of the system, it is important to know the damping rate induced by each swirler. One may assume that the system behaves like a second order system and deduce the damping rate value from the sharpness of the resonance curve using a standard half-power bandwidth method. This measurement is performed under cold flow conditions, in the absence of flame. This is admittedly a limitation of this determination but it is still important to have an estimate of the changes in damping rate that may be linked with the different swirlers.

For these measurements, the surroundings of the combustor are covered with an acoustic liner material to reduce unwanted reflections. The chamber length ($l_c = 165$ mm) for this measurement is chosen such that the resonance response occurs around the frequency of self-sustained instabilities in SICCA-spray. The chamber resonance occurs at a frequency $f_{\text{chamber}} \approx 460$ Hz, which corresponds to the quarter wave mode of the chamber. From the resonance curve, damping is calculated using the formula $\alpha = \pi \Delta f_r$ where Δf_r is the width of the resonance curve at half power (refer to Fig. 5(a)). The calculation of frequency response is performed using Welch's periodogram technique by considering two Hamming windows at each block with 50% overlap. This results in a frequency resolution of ± 1 Hz which in turn corresponds to a damping uncertainty of $\pm 3.14\,\text{s}^{-1}$. This measurement is performed for the three swirlers considered in this study, their frequency response is shown in Fig. 5(a) and the calculated damping values are indicated in Fig. 5(b). The damping rate is found to be about 90 s^{-1}, with some variation between the swirlers. The lowest value corresponds to the 712 swirler while the highest rate of damping is induced by the 716 unit. It is interesting to note that the swirler geometry influences this damping rate and that the variation in damping is of about 20% of the mean level.

Correlating the damping rate with the self-sustained measurements does not reason the observed instability behavior. For example, although 712 has the least damping rate at 460 Hz, it is almost

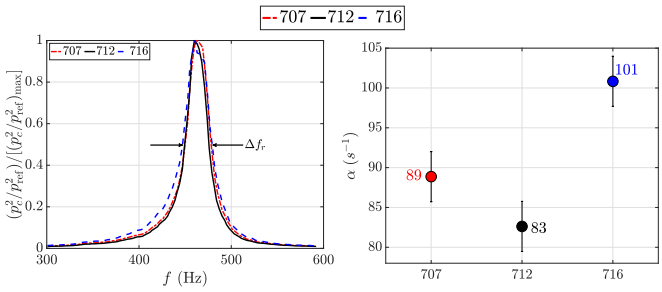

(a) Frequency response (b) Damping rate

Fig. 5: (a) Frequency response of SICCA-spray between 300 Hz to 600 Hz in cold flow conditions at $l_c = 165$ mm. Resonance occurs at a frequency of $f_{res} \approx 460$ Hz. (b) Calculated damping values ($\alpha = \pi \Delta f_r$) for the three swirlers. The error bars indicate the uncertainty in damping calculated from the frequency resolution in Welch's periodogram calculation which is equal to ± 1 Hz.

stable at this frequency (marked by gray diamond in Fig. 4). It is then instructive to measure flame describing function (FDF), which was also found to exhibit differences between the swirlers (not shown here). A theoretical framework can then be derived that accounts for the injector specific admittance and that provides linear instability bands. Using the FDF data, it is possible to retrieve some of the features described in the present article and in particular interpret the occurrence of self-sustained instability in SICCA-spray. Further results and interpretation of the data will be provided in a future article.

5 Conclusion

Experiments reported in this article underline the importance of the injection unit in combustion instability analysis. The present systematic investigation considers a fixed set of operating conditions, five combustion chamber lengths and three different swirlers but a fixed geometry of the upstream manifold and of the injector unit. It is first found that the three injectors establish flames that feature different mean shapes. The regimes of instability observed for these three swirlers do not occur for the same chamber length and they also differ in peak frequency and limit cycle amplitude level. The damping rates associated with the swirling injectors and determined from resonance experiments under cold flow conditions also change with a relative difference that may reach up to 20%. It is however worth noting that the damping rate is highest for the injector that also features high levels of oscillation. The interpretation of these experiments thus requires additional data concerning the different FDFs and a theoretical modeling including the injector admittance which will be reported in a future article.

Acknowledgements This work was partially supported by SafranTech (contract NF5Z-5100), by project FASMIC ANR16-CE22-0013 of the French National Research Agency (ANR), and by the European Union's Horizon 2020 research and innovation programme, Annulight with grant agreement no. 765998.

References

1. T. Poinsot, Proc. Combust. Inst. **36**(1), 1 (2017)
2. Y. Huang, V. Yang, Proc. Combust. Inst. **30**(2), 1775 (2005)
3. S. Candel, D. Durox, T. Schuller, J.F. Bourgouin, J.P. Moeck, Annual Review of Fluid Mech. **46**, 147 (2014)
4. C. Stone, S. Menon, Proc. Combust. Inst. **29**(1), 155 (2002)
5. D. Durox, J.P. Moeck, J.F. Bourgouin, P. Morenton, M. Viallon, T. Schuller, S. Candel, Combust. Flame **160**(9), 1729 (2013)
6. K.T. Kim, Combust. Flame **171**, 137 (2016)
7. G. Vignat, D. Durox, K. Prieur, S. Candel, Proc. Combust. Inst. **37**(4), 5205 (2019)
8. K. Prieur, D. Durox, T. Schuller, S. Candel, J. Eng. Gas Turb. Power **140**(3) (2018)
9. G. Vignat, D. Durox, A. Renaud, S. Candel, J. Eng. Gas Turb. Power **142**(1) (2020)
10. P. Rajendram Soundararajan, G. Vignat, D. Durox, A. Renaud, S. Candel, J. Eng. Gas Turb. Power, Online (2021)
11. G. Vignat, P. Rajendram Soundararajan, D. Durox, A. Vié, A. Renaud, S. Candel, J. Eng. Gas Turb. Power, Online (2021)